

Autonomous Oscillations in Carbon Monoxide Oxidation over Supported Rhodium

INTRODUCTION

Autonomous oscillatory states have been observed in many heterogeneous catalytic reaction systems (1) with carbon monoxide oxidation over platinum receiving the most attention (2). In order to elucidate the underlying sources of the oscillatory responses to time invariant inputs, several studies have been performed with reactions over supported catalysts in which transmission infrared spectroscopy was incorporated to measure IR active surface species. Particularly noteworthy are the findings presented by Kaul and Wolf (3–5) and Lindstrom and Tsotsis (6–8) for CO oxidation on supported Pt. Kaul and Wolf postulate the oscillations to be manifestations of surface nonuniformities and wave propagation of high reaction rate fronts, while Lindstrom and Tsotsis attribute mechanistic causes, specifically, oxidation and reduction of the Pt.

Few studies have reported oscillatory behavior in the reaction of CO with oxygen on rhodium (9–11). The aperiodic oscillations in CO₂ production reported by Franck *et al.* (9) coincided with large temperature fluctuations in the gas phase. Using a transmission IR reactor with a thin wafer of supported Rh, Prairie *et al.* (11) observed fluctuations in gas-phase and surface species which were not periodic. The purpose of the present work is to show oscillatory behavior observed for CO oxidation on Rh/Al₂O₃ that is quite different from that reported previously for this reaction. A transmission IR reactor was used so that oscillations in the surface species as well as

gas-phase species could be observed simultaneously. Therefore, the contribution of different adsorbed CO species to the overall dynamic behavior could be ascertained.

EXPERIMENTAL SYSTEM

Gas flow rates of carbon monoxide (99.99%), oxygen (99.5%), hydrogen (99.9995%), and helium (99.995%) into the reactor utilized a feed system described in detail by Prairie *et al.* (12). The reactor is based on a transmission IR cell design of Oh and Hegedus (13) and has been described elsewhere (14). Mounted in the reactor is an exposed-tip thermocouple bent to within 0.1 mm of the catalyst surface. The effluent concentration of either CO or CO₂ was measured with a Wilkes Miran I infrared analyzer operating at 4.6 or 4.2 μm, respectively. At 155°C and 100 sccm total flow rate, the reactor was found to yield an ideal CSTR response to a step change in the inlet concentration with a time constant of 3.8 s.

Transmission infrared spectra were obtained with a Beckman IR-8 infrared spectrophotometer modified to use a high-speed HgCdTe detector (Santa Barbara Research, Model 40742). In order to incorporate the HgCdTe detector, a high-speed chopper (Laser Precision, Model CTX-534) is placed in the sample beam and a lock-in amplifier (Princeton Applied Research) is coupled with the detector and chopper. This arrangement allowed for data to be taken only in single-beam mode. A monochromator slit width of 0.2 mm and a chopping speed of 400 Hz were used for all of the transmission IR spectra. An HP9825

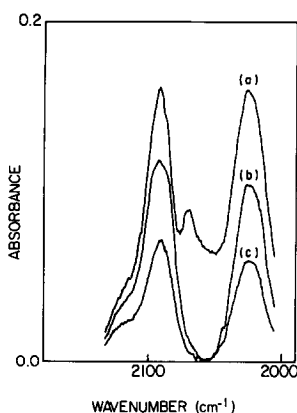


FIG. 1. IR spectra of CO on Rh/Al₂O₃ at 155°C: (a) saturated coverage, (b) 1 min after switch from CO to O₂, (c) 30 min after spectrum (b).

data acquisition system was used to store the effluent and surface IR data.

Rh/Al₂O₃ catalyst (5 wt%) was prepared from Alon fumed alumina and RhCl₃ using the aqueous incipient wetness technique. The catalyst powder was dried overnight and calcined for 5 h in flowing air at 500°C. Catalyst wafers were made by pressing the powder at 500 psi in a 20-mm-diameter die. Two catalyst wafers were used in the present study: one was 35 mg and 0.10 mm thick and the other was 22 mg and 0.07 mm thick. Prior to use, the wafers were each reduced *in situ* with 20% H₂ in He at 175°C for 10 h. Following hydrogen reduction with reactor was cooled to 155°C while flowing He through the cell. Before any carbon monoxide was introduced to the system a baseline spectrum was obtained.

RESULTS AND DISCUSSION

Figure 1a shows the spectrum resulting from introducing CO to the reduced catalyst at 155°C. The spectrum has been corrected for the baseline. Three absorbance bands that have been previously assigned to adsorbed CO species on supported Rh (15, 16) were observed. The doublet at 2090 and 2025 cm⁻¹ corresponds to the symmetric and asymmetric stretching modes, respectively, of CO adsorbed in a dicarbonyl

form. The band at 2070 cm⁻¹ is assigned to linearly adsorbed CO. No clear band was seen that could be attributed to a CO species adsorbed in bridged form.

To resolve the large amount of overlap between the absorbance bands, transient experiments were performed to determine the relative reactivity of the CO surface species. A transient was induced by a step change in the feed concentration from 4% CO in He to 5% O₂ in He at 155°C. Figure 2a shows the response of the effluent CO mole fraction to the step change. Also, shown in Figs. 2b and 3 are the time trajectories of the intensities of the 2070 and 2025 cm⁻¹ bands, respectively. The 2070 cm⁻¹ band intensity decreases to zero stepwise concurrently with the concentration of CO in the reactor approaching zero. The 2025 cm⁻¹ band displays a sharp decrease in intensity followed by a slower decline. The early rapid decrease in the 2025 cm⁻¹ band occurs simultaneously with the disappearance of the 2070 cm⁻¹ band. Consequently, this behavior at 2025 cm⁻¹ can be attributed

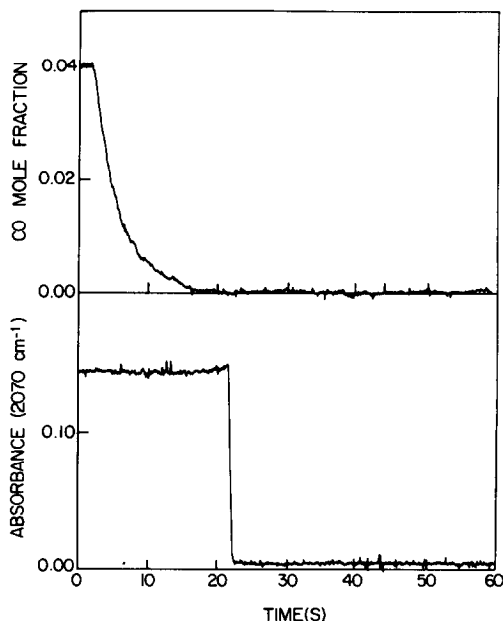


FIG. 2. Step change from 4% CO in He to 5% O₂ in He; (a) trajectory of the effluent CO mole fraction, (b) trajectory of the absorbance at 2070 cm⁻¹.

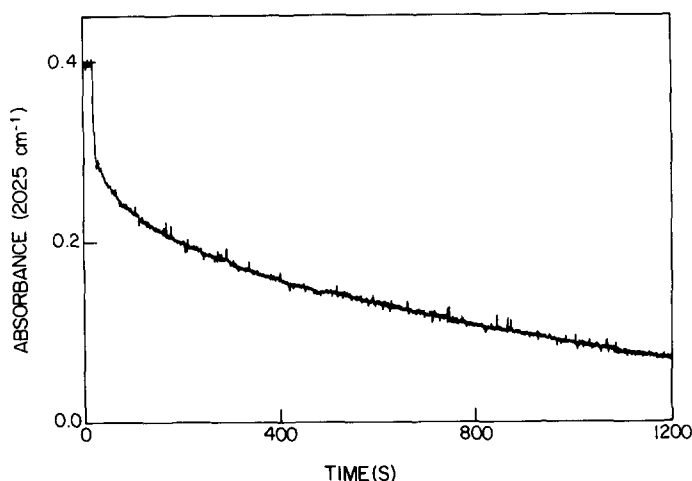


FIG. 3. Absorbance trajectory at 2025 cm^{-1} for switch from 4% CO to 5% O_2 .

to overlap between the absorbance bands. This effect on the full spectrum is illustrated in Fig. 1 where spectrum (b) was started 1 minute after the switch with a scan time of 20 s and spectrum (c) was taken 30 min later. All three of the spectra in Fig. 1 are shown after subtracting out the same baseline. As can be seen, the band corresponding to linearly adsorbed CO disappears within 1 min. Also, a shoulder at 2125 cm^{-1} becomes apparent. This band was previously assigned to CO and an oxygen atom bonded to the same Rh atom (15, 17). Figures 2b and 3 demonstrate that linearly adsorbed CO is more reactive than dicarbonyl CO at 155°C which agrees with a previous report by Yang and Garland (15) at a comparable temperature.

The response of the system containing the 35-mg catalyst wafer to a steady 100 sccm feed of 5% CO, 20% O_2 in He is shown in Fig. 4. Measurement of the intensity of the 2070 cm^{-1} band and of the effluent CO_2 mole fraction were performed simultaneously (Figs. 4a and 4b). Following this measurement the CO effluent concentration was monitored along with the 2070 cm^{-1} band. Although the effluent mole fractions of CO and CO_2 could not be measured simultaneously, these responses were in-phase, with high conversion corresponding

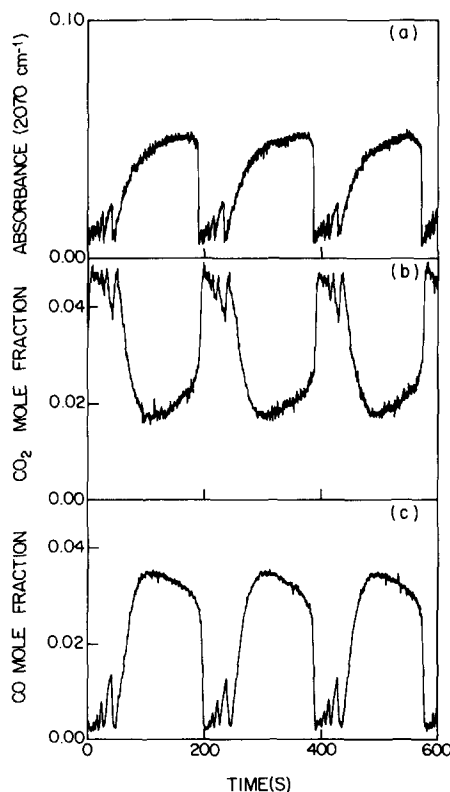


FIG. 4. Oscillations at 155°C for a steady feed of 5% CO, 20% O_2 : (a) absorbance at 2070 cm^{-1} , (b) effluent CO_2 mole fraction, (c) effluent CO mole fraction.

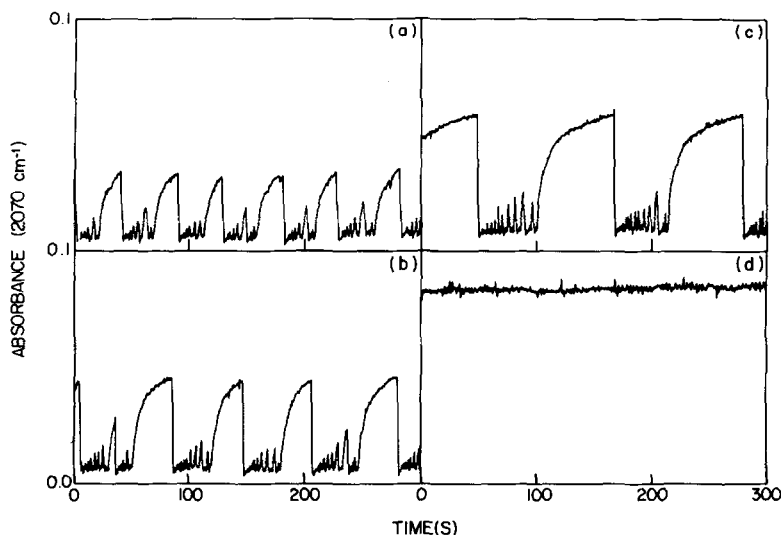


FIG. 5. Response of the absorbance at 2070 cm^{-1} for a feed composition of 2% CO and (a) 20% O_2 , (b) 15% O_2 , (c) 12% O_2 , (d) 10% O_2 .

to low linear CO coverage, because each was synchronized with the oscillations in the 2070 cm^{-1} band. During the oscillations, no temperature fluctuation was indicated by the thermocouple, although this in the gas phase measurement may not be sensitive to temperature excursions of the catalyst. The shape of the oscillations are very similar to those reported by Plichta and Schmitz (18) for CO oxidation on Pt foil. The instantaneous conversion of CO varied between 96 and 30% during the cycles, corresponding to reaction rates from 3.6 to $1.1\ \mu\text{mol/s}$. Based on observed quantities, the Thiele modulus (19) is approximately 0.55 and 0.01 for the high and low instantaneous reaction rates, respectively, based on quasi-steady state estimates.

Oscillations in-phase with the effluent CO measured response were observed while monitoring the absorbance at 2025 cm^{-1} . The absorbance at 2070 cm^{-1} decreased to nearly zero during the high reaction rate portion of the oscillations, indicating no linear CO on the surface. The absorbance at 2025 cm^{-1} remained substantial even during high conversion. Although the absorbances at the two wavenumbers

could not be monitored simultaneously, the response of the 2025 cm^{-1} band during the oscillations was very similar to that of the 2070 cm^{-1} band. These observations coupled with the reactivity results shown in Figs. 2b and 3 indicate that the primary cause of the oscillations measured at 2025 cm^{-1} is the overlap of the absorbance band for linear CO with the dicarbonyl band. A comparison between the time scale for removal of dicarbonyl by reaction with oxygen (Fig. 3) and the oscillation period shows that the contribution of the dicarbonyl species to the intensity at 2025 cm^{-1} remains essentially constant during the oscillations. Therefore, the oscillations cannot be primarily attributed to an interchange between linear CO and dicarbonyl species on the catalyst surface.

The effect of varying the inlet O_2 concentration is presented in Fig. 5. Shown is the absorbance at 2070 cm^{-1} for steady feeds of 2% CO and four O_2 concentrations: 20, 15, 12, and 10%. Each of the feed configurations that result in oscillations has a nearly equivalent high conversion level in a cycle but differs markedly in the maximum absorbance during a cycle and in the cycle

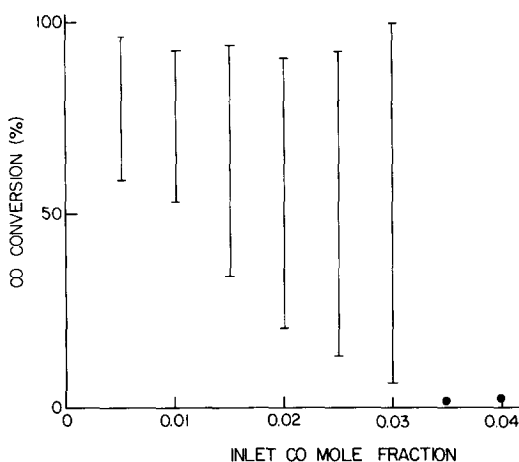


Fig. 6. Oscillatory behavior of the reaction at 155°C. Bands denote oscillation amplitudes, and solid circles denote stable steady states.

period. Decreasing the inlet O_2 concentration causes the absorbance to stay at a relatively high value for a longer portion of the cycle, until, as shown in Fig. 5d, the oscillations cease and the surface reaches saturation coverage.

The oscillatory behavior of the system with the 22 mg wafer is shown in Figs. 6 and 7 for two different reaction temperatures, 155 and 164°C. Plotted is the percentage conversion of CO for various inlet CO mole fractions and a fixed O_2 inlet mole fraction of 0.20. The solid circles represent stable

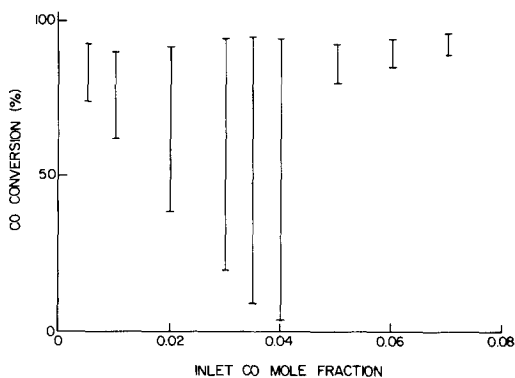


Fig. 7. Oscillatory behavior of the reaction at 164°C. Bands indicate the magnitude and maximum and minimum values of the oscillation.

steady states and the ends of the bands give the maximum and minimum instantaneous conversions during an oscillation. Due to limitations in the mass flow controllers, the minimum CO concentration that could be obtained accurately in the feed stream was 0.5%. At 155°C (Fig. 6), decreasing the inlet CO mole fraction from a stable steady state (solid circles) with low conversion caused the system to bifurcate to a large amplitude limit cycle. No hysteresis effect was observed as increasing the CO mole fraction from 0.03 to 0.035 caused the system to return to the low conversion state. In contrast, increasing the inlet CO concentration from the large amplitude oscillatory regime at 164°C forced the system to an oscillatory state of small amplitude and high conversion. Again, no hysteresis was observed switching between the large and small amplitude oscillations. Figure 8 shows the oscillations in the effluent CO mole fraction resulting from a feed of 5% CO, 20% O_2 at 164°C. The oscillations are not periodic as were observed for the large amplitude oscillations but were still correlated between the effluent CO mole fraction and the absorbance at 2070 cm^{-1} .

Figures 6 and 7 provide insight into a possible contributing factor to the large amplitude oscillations. While increasing the CO mole fraction at 155°C caused the oscilla-

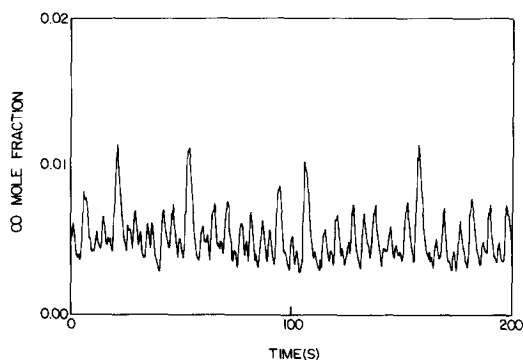


Fig. 8. Small amplitude oscillations in the effluent CO mole fraction at 164°C with feed composition of 5% CO, 20% O_2 .

tions to quench to a low conversion state, the system moved to a high conversion value at 164°C. If the catalyst surface is being locally heated by chemical reaction, but this heating is undetected by the thermocouple, then ignition and extinction may be occurring between the low and high conversion states as the crystallites heat and cool. The pebbly surface model proposed by Jensen and Ray (20) could be used to explain the complex behavior shown in Fig. 8, but the long-time scale oscillations in Fig. 4 are difficult to reconcile with this model. Oscillations with periods of approximately 7 min were reported by Lynch and Wanke (21) for CO oxidation on Pt-Pd/Al₂O₃ which were postulated to coincide with surface temperature fluctuations rather than independent crystallite vacillations.

Although the precise oscillatory mechanism has not been isolated, it is apparent that neither interchange between linear CO and dicarbonyl species nor a change in the fractional coverage of CO adsorbed in the dicarbonyl form occurs during the oscillations. Rice *et al.* (17) have presented data indicating dicarbonyl species occur on Rh in a +1 oxidation state while linearly adsorbed CO corresponds to Rh in a zero oxidation state. Using the interpretation of Rice *et al.*, the oscillatory data here do not confirm a change in the oxidation state of the rhodium during the oscillations. The data presented in this work do suggest that temperature fluctuations appear to be a likely contributor to the oscillatory behavior observed in this reaction system.

ACKNOWLEDGMENT

This work was supported by the National Science Foundation.

REFERENCES

1. Chang, H.-C., in "Dynamics of Nonlinear Systems" (V. Hlavacek, Ed.), p. 85. Gordon & Breach, New York, 1986.
2. Razon, L. F., and Schmitz, R. A., *Catal. Rev.-Sci. Eng.* **28**, 89 (1986).

3. Kaul, D. J., and Wolf, E. E., *J. Catal.* **89**, 348 (1984).
4. Kaul, D. J., and Wolf, E. E., *J. Catal.* **91**, 216 (1985).
5. Kaul, D. J., and Wolf, E. E., *Chem. Eng. Sci.* **41**, 1101 (1986).
6. Lindstrom, T. H., and Tsotsis, T. T., *Surf. Sci.* **150**, 487 (1985).
7. Lindstrom, T. H., and Tsotsis, T. T., *Surf. Sci.* **167**, L194 (1986).
8. Lindstrom, T. H., and Tsotsis, T. T., *Surf. Sci.* **171**, 349 (1986).
9. Franck, K. R., Lintz H.-G., and Tufan, G., *J. Catal.* **79**, 466 (1983).
10. Tufan, G., and Lintz, H.-G., "Proceedings, 5th International Symposium on Heterogeneous Catalysis, Varna," Part II, p. 79, 1983.
11. Prairie, M. R., Oh, S. H., Cho, B. K., Shinouskis, E. J., and Bailey, J. E., submitted for publication (1987).
12. Prairie, M. R., Shanks, B. H., and Bailey, J. E., *Chem. Eng. Sci.*, in press (1988).
13. Oh, S. H. and L. L. Hegedus, in "Catalysis under Transient Conditions" (A. T. Bell and L. L. Hegedus, Eds.), Vol. 178, p. 79. ACS Symp. Ser., Washington, DC, 1982.
14. Prairie, M. R., Ph.D. thesis, California Institute of Technology, 1987.
15. Yang, A. C., and Garland, C. W., *J. Phys. Chem.* **61**, 1504 (1957).
16. Yates, J. T., Duncan, T. M., Worley, S. D., and Vaughan, R. W., *J. Phys. Chem.* **70**, 1219 (1979).
17. Rice, C. A., Worley, S. D., Curtis, C. W., Guin, J. A., and Tarrer, A. R., *J. Chem. Phys.* **74**, 6487 (1981).
18. Plichta, R. T., and Schmitz, R. A., *Chem. Eng. Commun.* **3**, 387 (1979).
19. Aris, R., "The Mathematical Theory of Diffusion and Reaction in Permeable Catalysts," Vol. 1. Oxford Univ. Press, London, 1975.
20. Jensen, K. F., and W. H. Ray, in "Dynamics of Nonlinear Systems" (V. Hlavacek, Ed.), p. 111. Gordon & Breach, New York, 1986.
21. Lynch, D. T., and Wanke, S. E., *J. Catal.* **17**, 345 (1984).

BRENT H. SHANKS
JAMES E. BAILEY

Department of Chemical Engineering
California Institute of Technology
Pasadena, California 91125

Received July 14, 1987